Nanoscale

Randomly nano-structured scattering layer as an internal light-extracting layer for transparent organic light emitting diodes

Journal:	*Nanoscale*
Manuscript ID:	NR-ART-03-2014-001520.R1
Article Type:	Paper
Date Submitted by the Author:	13-Jun-2014

Complete List of Authors:	Huh, Jin Woo; Electronics and Telecommunications Research Institute, Convergence Components Materials Research Laboratory Shin, Jin-Wook; Electronics and Telecommunications Research Institute, Convergence Components Materials Research Laboratory Cho, Doo-Hee; Electronics and Telecommunications Research Institute, Convergence Components Materials Research Laboratory Moon, Jaehyun; Electronics and Telecommunications Research Institute, Convergence Components Materials Research Laboratory Joo, Chul Woong; Electronics and Telecommunications Research Institute, Convergence Components Materials Research Laboratory Park, Seung Koo; Electronics and Telecommunications Research Institute, Convergence Components Materials Research Laboratory Hwang, Joohyun; Electronics and Telecommunications Research Institute, Convergence Components Materials Research Laboratory Cho, Nam Sung; Electronics and Telecommunications Research Institute, Convergence Components Materials Research Laboratory Lee, Jonghee; Electronics and Telecommunications Research Institute, Convergence Components Materials Research Laboratory Han, Jun-Han; Electronics and Telecommunications Research Institute, Convergence Components Materials Research Laboratory Chu, Hye Yong; Electronics and Telecommunications Research Institute, Convergence Components Materials Research Laboratory Lee, Jeong-Ik; Electronics and Telecommunications Research Institute, Convergence Components Materials Research Laboratory

Cite this: DOI: 10.1039/c0xx00000x

www.rsc.org/xxxxxx

PAPER

Randomly nano-structured scattering layer as an internal light-extracting layer for transparent organic light emitting diodes

Jin Woo Huh, Jin-Wook Shin, Doo-Hee Cho, Jaehyun Moon, Chul Woong Joo, Seung Koo Park, Joohyun Hwang, Nam Sung Cho, Jonghee Lee, Jun-Han Han, Hye Yong Chu and Jeong-Ik Lee*

Received (in XXX, XXX) Xth XXXXXXXXX 20XX, Accepted Xth XXXXXXXXX 20XX
DOI: 10.1039/b000000x

A random scattering layer (RSL) consisting of a random nano-structure (RNS) and a high refractive index planarization layer (HRI PL) is suggested and demonstrated as an efficient internal light-extracting layer for transparent organic light emitting diodes (TOLEDs). By introducing RSL, remarkable enhancement of 40% and 46% in external quantum efficiency (EQE) and luminous efficacy (LE) was achieved without causing deterioration in the transmittance. Additionally, with the use of the RSL, viewing angle dependency of EL spectra was reduced to a marginal degree. The results were interpreted as the stronger influence of the scattering effect over the microcavity. The RSL can be applied widely in TOLEDs as an effective light-extracting layer for extracting the waveguide mode of confined light at indium tin oxide (ITO) / OLED stack without introducing spectral changes in TOLEDs.

Introduction

Practical out-coupling efficiency in transparent organic light-emitting diodes(TOLEDs), when the emission through only one side is counted, is lower than that of conventional bottom emissive OLEDs. Furthermore, even the total efficiency considered in both bottom and top sides of TOLEDs, at best, currently reach only 70~80% of corresponding bottom emissive OLEDs. In addition, fundamentally, the light out-coupling efficiency for an OLED with a flat glass substrate is limited to ~20%.[1, 2] Therefore, improvement of the out-coupling efficiency in TOLEDs is more serious issue than that in the conventional OLEDs.

In general, the out-coupling losses are caused by surface plasmon polaritons (SPPs) at an metal-organic interface, waveguide mode in an ITO/organic layer, and substrate mode in a glass substrate. Particularly, a significant portion(~60%) of generated light is confined within the substrate mode and the waveguide mode due to total internal reflection(TIR).[2] While loss of the substrate mode can easily be recovered by attaching a commercial micro lens array or a light extraction film on the surface of the substrate, the light extraction of the waveguide mode is much more challenging to achieve[3-5] because it requires a modification of the internal structure inside the device. Hence, various designs and techniques for enhancing light extraction of the waveguide mode have been proposed, including substrate surface modifications,[6, 7] low-index grids,[8] and Bragg diffraction gratings.[9–11]

As trials for enhancing light extraction in TOLEDs, Choi et al.[12] suggested the periodically perforated WO3 layer to apply in TOLEDs for light extraction. Inspite of its effectiveness in improving outcoupling efficiency with optical clarity in the TOLEDs, the WO3 layer showed EL spectral changes at specific wavelength satisfying the Bragg diffraction condition caused by periodic structure. To overcome these changes in spectrum or CIE color coordinates, Kim et al.[13] at the same group introduced WO3 nanoislands and they exhibted it induced invariance of spectrum changes and no specific angular dependency. However, they focused on bottom-emissive OLEDs. Research to achieve transmittance for its application to TOLEDs still remains unresolved. Recently, Chang et al.[14,15] proposed nanoparticle-based scattering layer(NPSL) to stabilize the spectral depedency on viewing angle of the outcoupled light. Although NPSL has shown to be highly effective as a light extraction structure for white OLEDs,[14] TOLEDs with NPSL called as NPSL-based bi-directional OLEDs have very low transmittance due to its very high haze of 85%,[15] which is not suitable for TOLEDs.

In this work, we suggest random nano-structure (RNS) as new approach to improve both out-coupling efficiency and spectral angular independency without compromising transmittance in TOLEDs. In order to achieve our goal, first, RNS was fabricated to have random. Second, light extraction in TOLEDs equipped with RNS was optimized by adjusting microcavity length. In this course the the thicknesses of the hole transport layer(HTL) and electron transport layer(ETL) were varied. Microcavity and scattering effects by OLED-stack structure were investigated by varying HTL thickness using both computer simulations(2- and 3-dimension) and experiments. As a result, total efficiency was

remarkably enhanced without introducing spectral-change over viewing angle and no significant decrease in transmittance. The mechanism of light extraction in the suggested structure of TOLED was also investigated.

Experimental details

Random scattering layer(RSL) and the RSL embedded TOLED

Figure 1a and 1b shows the TOLED structures we used. One was equipped with an RNS and the other not. The RNS cannot be applied directly in the TOLED because its rough surface deteriorates electrical characteristics of the OLED device. Thus, we coated a high refractive index planarization layer(HRI PL) composed of TiO_2 on the RNS as seen as fig 1c. We call the layer composed with a RNS and a HRI PL as a random scattering layer(RSL). The preparation of the RSL has been previously reported.[16] The scattering layer consists of irregular nano-sized pillars which have heights of ~350nm and diameters of 200~500nm. A ~ 1μm-thick planarization layer was formed on the nano pillars. The planarization layer has a high refractive index (n) of 2.02 at 550 nm. It is important of choosing a planarization material which has higher n than ITO, otherwise a big fraction of the generated light will undergo total internal reflection.

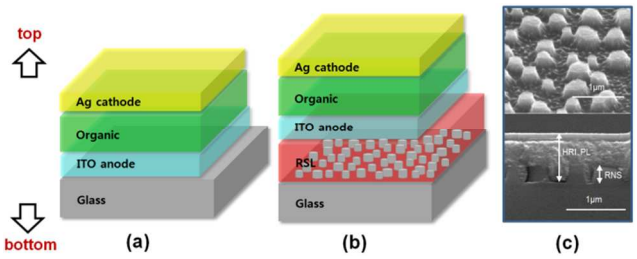

Fig 1. Structures of the TOLEDs (a) w/o and (b) w/ the RSL. (c) SEM images of RNS (top) and cross section of RSL (bottom)

The TOLED we fabricated has green-colored emission with its main peak at λ = 540 nm. The stack of the TOLED we fabricated is as following; Indium Tin Oxide (ITO) (100nm) / 1,1-Bis[(di-4-tolylamino)phenyl] cyclohexane (TAPC) (100, 160, 230nm) / 4,4',4"-Tris(N-carbazolyl)-triphenylamine (TCTA) (5nm) / Phosphorescent emission layer (10nm) / 2,6-Bis(3-(carbazol-9-yl)phenyl) pyridine (DCzPPy) (10nm) / 1,3-Bis(3,5-di-pyrid-3-yl-phenyl)benzene (BmPyPB) (40nm) / LiF (1nm) / Al (1.5nm) / Ag (15nm) / TAPC (120nm). Based on the results of our previous report,[17,18] we introduced TAPC of 120nm as a capping layer(CL) on the Ag cathode to maximize total efficiency by enhancing reflectance of the cathode. The fabrication processes have been described in our previous works.[19] We basically fabricated the TOLEDs with an emitting area of $1.5\times1.5mm^2$ to measure current-voltage -luminescence (I-V-L) characteristics of the devices. In order to capture the scattering feature, the luminance values were measured as a function of viewing angle. Later, the values were integrated to obtain an overall performance for a given TOLED. In this course we have used devices with active area of $7x10mm^2$ for collecting angularly integrated values and measured the emission as a function of angle. External quantum efficiency (EQE) and luminous efficacy (LE) was calculated by integrating angular and spectrally resolved emissions. The electroluminescence spectrum was measured using a Minolta CS-2000. The I-V-L characteristics were obtained with a source/measure unit (Keithley 238) and a Minolta CS-100. Transmittance was measured using an UV-visible spectrophotometer (U-3501, Hitachi). Additionally, transmission haze and total transmittance were measured using haze meter (haze-gard plus, BYK Additives & Instruments).

Computer simulations

To deduce experimental conditions for investigating the microcavity effects in the TOLED, we performed simulations using a commercial OLED optical simulator, SimOLED.[20,21]

The scattering effects of RSL were also investigated using a three dimensional (3D) finite-difference time-domain (FDTD) simulation method.[22,23] The size of computational domain was 8μm x 8μm x 10μm, where the last dimension refers to the direction perpendicular to the OLED layers. The spatial resolution in FDTD calculation was 20nm. In order to effectively mimic the OLED light source, we have constructed an emitting layer which consists of distributed dipole sources. The dipoles sources have orthogonal x-, y-, z-polarizations and a central wavelength of 540 nm. For RNS, numerous nano-pillars with a height of 350nm and a diameter range of 200~500nm were randomly distributed on the substrate. Based on the microstructural observations, the spacing between nano pillars were chosen to have a range of 50~500 nm. From the FDTD simulations, we obtained far field (E^2-intensity) profiles and their integrated values, which are being plotted on a hemispherical surface detector. In order to obtain realistic simulation results, we used all measured optical constants (n, k) of organic materials, which were measured using an ellipsometer (M-2000D, J. A. Woollam Co.).

Results and Discussion

Optical effect of RSL

In order to investigate the microcavity effect, the scattering layer was treated as a homogeneous single layer without any scattering structure (fig 2a,2b). Subwavelengh features were used to obtain an effective refractive index.[24,25] This TOLED was compared with the reference TOLED which has no RSL between the glass and the ITO. In the reference device, the microcavity forms between the Ag cathode and the ITO anode. However, in TOLEDs with the RSL, due to the high optical contrast between the RSL and the glass, microcavity takes place between the Ag cathode and the RSL.

Fig. 2c exhibits simulated result of cavity effect dependent on HTL thickness. The thickness of ETL was fixed as 40 nm based on our preliminary simulation results (see Supplementary) and the thickness of HTL was varied in a range of 0~300nm in simulations. The total radiances in bottom and top direction in both devices show periodic oscillation depending on the HTL thickness due to resonance. The radiance has maximum and

minimum at a specific HTL thickness: in TOLEDs with the RSL, the highest total radiance was obtained at the thickness range of 60~80nm (the first order) and 220~240nm (the second order); the lowest was observed near 160nm. The period in TOLEDs with the RSL is ~170nm and similar to that in the ref. device, but its phase is shifted behind the reference TOLED. This phase change might be induced from the change of reflection at bottom side in cavity structure of RSL-embedded device.[26] In fig. 2c, remarkable change to be worthy of notice is that the resonance in the TOLED with the RSL is considerably weakened relative to that of the reference TOLED, while strong cavity is sustained in the reference device.

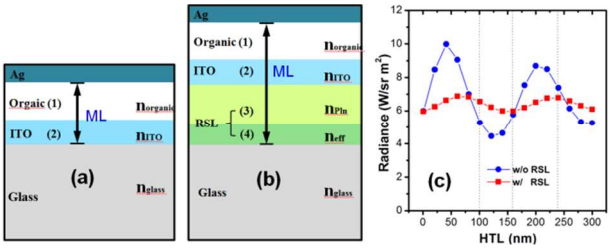

Fig.2. Schematic diagrams of the TOLED structures (a) w/o and (b) w/ the RSL, and (c) their simulated results as a function of HTL thickness (Arrows designate structure where microcavity forms.)

This simulated result can be interpreted by the change in the microcavity on optical length and coherence in the device structure. The total optical length of the microcavity (ML) in OLED with multi-layer structure is given [27, 28] by

$$ML = \sum n_i d_i + | (\varphi_m \lambda)/(4\pi) | \quad (1)$$

where n_i and d_i are the refractive index and thickness of the i-th film layer. φ_m is the phase shift at the Ag cathode reflector and λ is the free-space wavelength. In Eq. (1), the second term, which is the effective penetration depth into the top metal mirror, is usually small in comparison to the first term.[28] Hence ML can be approximated as the first term, the sum of the optical thicknesses of the layers. Parameters relevant to our work and calculated ML are listed in table 1. The table shows that the microcavity lengths in the TOLEDs w/o and w/ the RSL are about 0.3~0.8μm and about 2.2~2.8μm, respectively. In addition, to investigate the optical effect of the planarization layer without RNS, we also calculated ML, of which results are summarized in Table 1. The calculation result shows that the ML in the TOLED equipped with only HRI PL is more or less the same to that TOLED equipped with RSL. This results strongly suggest that the ML in the device with RSL is dominated by the HRI PL. If PL is applied only without RNS in OLEDs, the cavity length increases monontonically due to its similarity in refractive index to that of ITO, additionally, internal absorption is expected to increase through the thick layer of the PL.

Table 1. Refractive index and thickness of each layer in the TOLED structures w/ and w/o the RSL, and w/ only HRI PL.

	Materials	Refractive index (n_i)	Thickness (d_i) (μm)	n_i x d_i (μm)		
				w/o RSL	w/ RSL	w/ HRI PL
1	Organic	1.76	0.065~0.365 (HTL:0~0.3)	0.11~0.64	0.11~0.64	0.11~0.64
2	ITO	1.98	0.100	0.20	0.20	0.20
3	HRI PL	2.02	1.000			2.02
		2.02	0.650		1.31	
4	RNS + HRI PL	1.76	0.350		0.62	
Total(∑) ML				0.31~0.84	2.24~2.77	2.33~2.86

Coherence in typical OLED structure maintains to some degree since the total film thickness in the structure is not longer than the wavelength of emissive light. However, in the RSL-embedded OLED structure, we should consider coherence length[29] because the total thickness exceeds the visible wavelength range. Moreover, the resonance of light waves can only arise over the coherence length in cavity structure. The coherence length is approximated by $\lambda^2/\Delta\lambda$ [29,30] where λ, and $\Delta\lambda$ are light wavelength and full-width at half maximum, respectively. From the formula, using λ=540nm and $\Delta\lambda$=80nm in emitted light, the coherence length of the emitted light in two devices was calculated as about 3.7μm. This means that the microcavity length in the device with RSL or only HRI PL is comparable to the coherence length, thus the degree of microcavity effects is considerably lessened compared to that of the reference device. Accordingly, the overall OLED light output is expected to be proportional to the cavity extent.[26,31,32] This cavity effect of RSL in the device is confirmed in the simulations (fig. 2c).

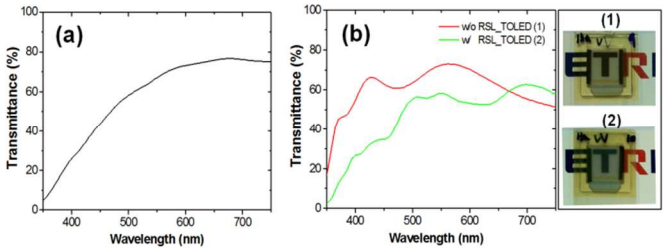

Fig 3. Transmittance of (a) the substrate w/ the RSL and (b) the TOLEDs w/ and w/o the RSL

Performance of TOLEDs with RSL

In order to verify optical effect on the HTL thickness and light extraction effect on the RSL in TOLEDs, we fabricated green TOLED device with and without the RSL. In particular, we paid attention to the influence of microcavity design. Based on simulation results, we chose three thicknesses of HTLs, which correspond to maximum (230 nm), minimum (160 nm) and midpoint (100 nm) peaks in the radiance variation. To avoid the occurrence of internal-short circuit, which can be caused by

protruding parts of nano pillars, we intentionally chose HTL thicker than 100 nm.

The transmittance of ITO substrate with the RSL was shown in figure 3a. Transmittance is ~60% at 500nm and reaches at 70~80% above the region of 550nm. In this substrate, haze was measured as ~15%, which is due to light scattering by the nano-sized pollars. When the substrate with the RSL is embedded in the TOLEDs (Fig.3b), the transmittance of the device maintains 55~60% above the region of 500nm although the transmittance in the region below ~500nm is relatively low. The low transmittance in the wavelength region shorter than 500 nm might be caused by the diffusion of light due to maximization of scattering because the wavelength is comparable to the size of nano pillars. Total transmittance (TT), sum of direct (Fig.3b) and diffuse transmittances, was measured as up to ~70 %. Though scattering attributed to RSL in TOLEDs brings about haze and decreases direct transmittance, it contributes to diffuse transmittance and increases TT after all. This strongly indicates that the RSL can spread light over wide wavelength range without serious absorption loss. Such feature is of prime importance in the field of internal light extraction. The pictures in the figure 3b show actual images of TOLEDs. In both cases, the letter "T" is clearly discernible without blur.

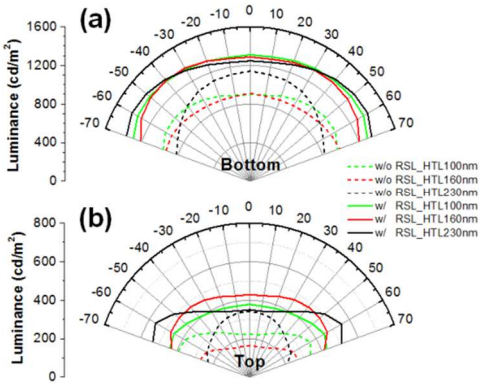

Fig.4. Angular distribution of luminance in (a) bottom and (b) top directions

Fig.4 shows the bottom and top angular distributions of luminance as a function of HTL thickness. The luminance was measured at a constant current density of 2mA/cm^2. In the case of the device without the RSL, the effect of microcavity can be clearly observed. The microcavity designed OLED with a HTL thickness of 230 nm showed higher bottom and top luminance than those with 100 nm and 160 nm HTL thicknesses at normal direction (θ=0^o). However, in the case of the RSL embedded devices, the luminance profiles were very similar each other irrespective of the HTL thickness. In addition, insertion of the RSL was observed to have an effect of enhancing luminance uniformly without preference to specific viewing angle. We attribute those features to the strong scattering effect of the RSL and alleviated microcavity effect This observation is particularly evident in the bottom emissions rather than top emission. Thus, more significant improvement is achieved in the bottom-side emission. The difference in bottom and top emissions will be discussed using the EL spectra. Our approach suggests an effective method for extracting the waveguide mode of confined light at ITO/OLED stack and spreading out the light in a diffusive fashion. The process and mechanism for light extraction of waveguide mode will be described in the following .

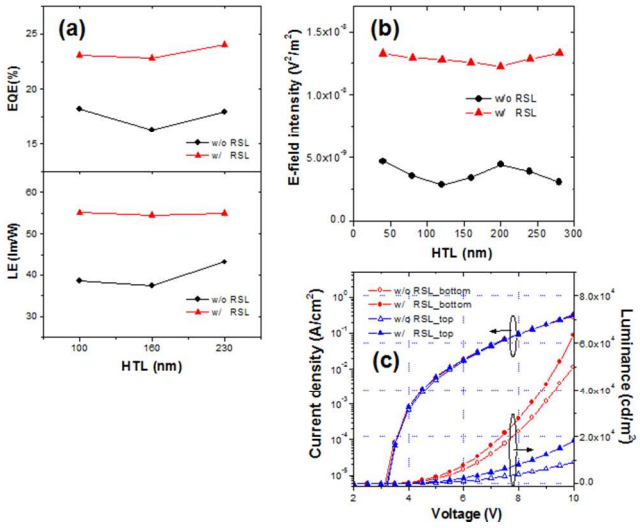

Fig. 5 (a) EQE and LE and (b) FDTD-simulated data depending on HTL thickness in the TOLEDs w/ and w/o the RSL. (c) J-V-L characteristics in the TOLEDs with the RSL (under HTL thickness of 160nm)

Evaluated total external quantum efficiencies (EQEs) and luminous efficacies (LEs) as seen in Fig. 5 support these discussions. With the RSL, it was observed that the total EQE increased to ~22~24% with enhancement of ~27~40%, and also the total LE improved up to ~55lm/W with enhancement of ~28~46% (Fig 5a). It is noticeable that the EQEs and LEs of the RSL embedded TOLEDs improved to a very similar level with showing rather weak dependency on the HTL thickness. However the microcavity effect is significant in the reference TOLEDs as mentioned above. These observations were clearly reproduced in the FDTD simulations on the far field radiation (Fig. 5b).

Oscillatory behavior in the far field radiation in the reference TOLEDs is almost flattened out in the RSL embedded TOLED. Agreements between the simulated and measured data can be observed in their EQE and LE dependency on the HTL thickness. From practical view point, the dominancy of scattering and weak dependency of microcavity is very useful in light extraction design. When we use the RSL in the TOLEDs, the TOLED with 160 nm HTL corresponding to the thickness of the minimum radiance shows almost same EQE and LE values as the TOLED with optimized HTL thickness corresponding to the maximum radiance. Accordingly, the highest light extraction enhancement was achieved in the device with the HTL thickness of 160nm. The total increments in EQE and LE were 40 % and 46%, respectively. Table 2 summarizes measured total EQE and LE values of each TOLED.

Fig. 5c shows the J-V-L (Current density-Voltage-Luminance) characteristics of TOLEDs with the RSL in case of HTL thickness of 160nm. The L-V plot displays that the TOLED with

the RSL showed distinct improvement in the luminance of bottom and top sides compared to the reference TOLED. However, in the J-V plot, two devices showed almost identical current density-voltage characteristics. Referring to J-V-L measurements, we can draw a conclusion that the RSL induced luminance enhancement is purely optical not electrical.

Table 2. External quantum efficiency and power efficiency of the TOLED w/ and w/o the RSL.

HTL(nm) (ETL40nm)	External quantum efficiency (%)			Luminous efficacy (lm/W)		
	w/o RSL	w/ RSL	Enhancement	w/o RSL	w/ RSL	Enhancement
100	18.2	23.1	26.9%	38.4	55.1	43.5%
160	16.3	22.8	39.9%	37.3	54.5	46.1%
230	18.0	24.0	33.3%	43.1	55.0	27.6%

The effect of introducing the RSL on the electro-luminescence (EL) spectra was shown in Fig 6. The EL spectra were collected from the normal viewing angle ($\theta=0^o$). All EL spectra in bottom and top side were normalized. Arrow spans in the graph of fig 6a designate minimum and maximum of Full Width at Half Maximum (FWHM) in spectra of TOLEDs with different HTL thickness.

When the RSL is absent, the FWHM changes considerably as the HTL thickness changes. With the introduction of the RSL, the difference in the FWHMs diminishes compared to the reference TOLED, which may be attributed to dominancy of scattering effect over optical microcavity effect. In bottom side**,** presumably due to the scattering dominancy, the FWHM tend to be slightly wider because introduction of the RSL causes microcavity effect to abate. Meanwhile peak-distortions or -shifts were observed to appear in top side EL spectra. Particularly at the HTL thickness of 230nm where cavity effect was maximized from simulated result, spectral peak position and shape were changed considerably. Recalling the measurement results of Fig. 4, the EL spectra in top side are understood as a combination scattering and microcavity effects. The corresponding two factors may be described as following. First, the scattering effect in the top side is originated only from the light component reflected from the RSL which is located at the bottom side. Second, in our structure, the CL of 120nm plays a role of maximizing reflectance at the top side,[13] leading to strengthen microcavity effects. Therefore, contribution of scattering is weaker than that of microcavity in the top emission due to above two factors.

Figure 6c illustrates our interpretation on the optical phenomenom inside the TOLED with the RSL and describes light extracion mechanism. In the figure, we assume identical emission of $^{D}E_o$ and $^{U}E_o$, which originate from the emissive organic layer. When the emitted light of $^{D}E_o$ encounters the RSL, scattering toward bottom and top direction occurs. In the case of the bottom direction, the scattered light components toward substrate primarily contribute to scattering effect: the $^{D}E_o(S_D)$ (Scattered light of $^{D}E_o$ toward bottom side), $^{UI}E_R(S_D)$ (Scattered light of $^{UI}E_R$ which is the reflected light of $^{U}E_o$ from the lower part of CL), and $^{UII}E_R(S_D)$ (Scattered light of $^{UII}E_R$ which is the reflected light of $^{U}E_o$ from the upper part of CL). This scattering effect at the bottom side can be understand as a random diffraction event which faciliactes the outcopuling of the confined light at the glass/ITO interface and ITO-organic stacks. However, If light is initially scattered toward top side by diffusive reflection from the RSL($^{D}E_o(S_U)$), the reflected lights of $^{D}E_o(S_U)$ from the CL(see dotted lines in figure 6c)) indirectly contribute to light extraction of the waveguide mode for bottom emission. Meanwhile, for the top side emission, the scattering effect in top side originates only from the diffusively reflected lights ($^{D}E_o(S_U)$...) from the RSL. Although there may be additional sequential scattering toward top side by reflection, the scattering effect is negligible.

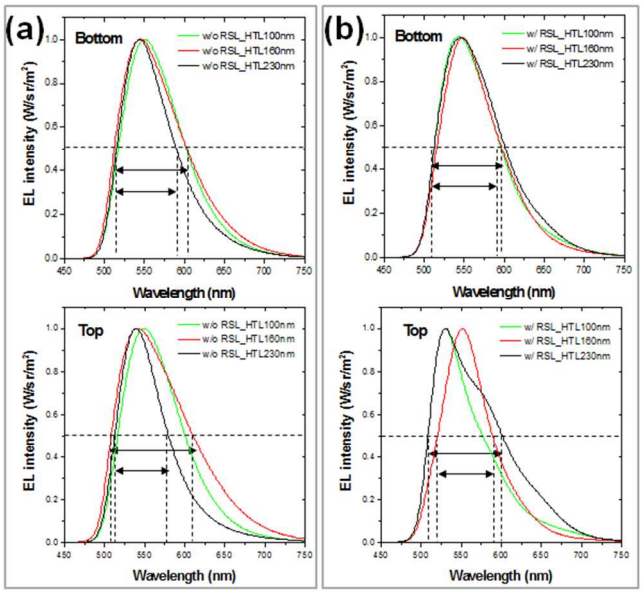

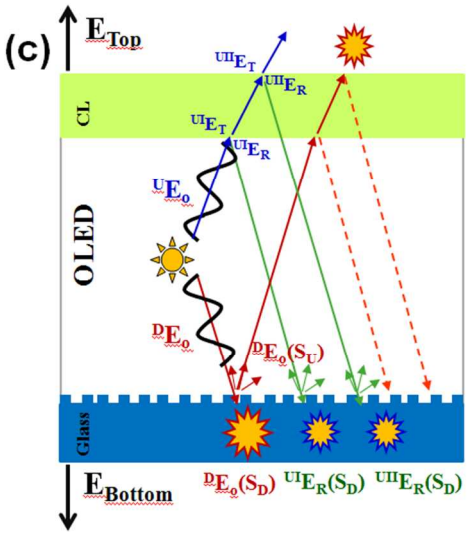

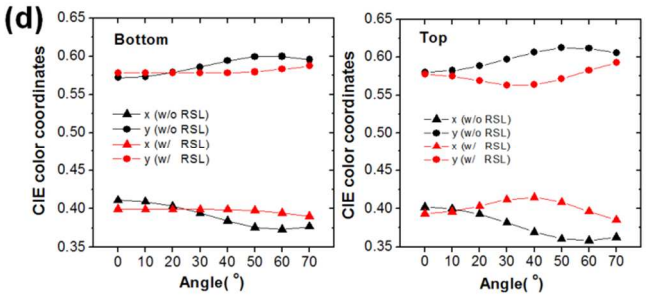

Fig.6. Comparison of the emission between the TOLEDs (a) w/o and (b) w/ the RSL in bottom and top sides, respectively. (c) Schematics of emissive light components in the TOLEDs w/ the RSL. (d) CIE color coordinates vs. viewing angle in the TOLEDs w/o and w/ the RSL (under the HTL thickness of 230nm)

These overall processes indicate that scattering effect in bottom side is stronger than that in top side. Conversely, in the top emission the microcavity effect is more apparent. The bigger enhancement in the bottom-side emission arises from the direct extraction of waveguide mode in ITO-organic stack due to strong scattering. The relatively small enhancement of the top side emission is due to the randomly reflected light components from the RSL layer. Furthermore, the high reflectance of the CL gives boost to the bottom emission and yields a bottom/top emission ratio of ~ 5.[17] The CL enhances microcavity, which may cause distortion in the EL spectra. Our results in fig 6a and 6b show that the RSL has a function of relieving spectral dependency by averaging the light traveling paths, resulting in suppressed microcavity effect and spectral stability.

Figure 6d shows the Commission Internationale de l'Eclairage (CIE) coordeinates as a function of viewing angle. The HTL thickness is 230 nm, which corresponds to a strong microcavity condition. The TOELDs with the RSL have lower variation in the CIE coordinates. This trend is more obvious in the bottom emission than top emission. As the angle changes from 0^o to 70^o, CIE (Δx, Δy) of the reference TOLED in bottom and top sides are (0.038, 0.028) and (0.044, 0.317), respectively. In the RSL equipped device, as the angle changes from 0^o to 70^o, the CIE (Δx, Δy) in bottom and top sides are (0.009, 0.009) and (0.003, 0.029), respectively.

In addition, the introduction of the RSL scarcely changes the color coordinate. The differences in the normal direction ($\theta=0^o$) CIE coordinates between with and without the RSL were achieved within Δ(0.02, 0.02)(bottom) and Δ(0.05, 0.04)(top) in all HTL thicknesses. With the use of HTL thickness 160 nm the color change due to introduction of the RSL was extremely small. The CIE coordinates vary negligibly as Δ(0.005, 0.007) and Δ(0.01, 0.02) in bottom and top emissions, respectively.

Conclusions

In conclusion, we fabricated transparent OLEDs (TOLEDs) with internal nano-structured random scattering layer (RSL) and demonstrated the RSL as an internal light-extracting layer to improve both efficiency and spectral viewing angle independency. The average transmittance of the TOLEDs with the RSL was ~57% and the haze was ~15%, which were comparable to TOLEDs without the RSL. The use of the RSL showed remarkable enhancements of ~40% and 46% in external quantum efficiency (EQE) and luminous efficacy (LE), even the haze of TOLEDs with the RSL was not high. The EQE and LE reached ~24% and ~55 lm/W, respectively. Optical effects in the internal structure of TOLEDs were also investigated as a function of HTL thickness with simulations and experiments. Without the RSL the out-coupling of TOLED is governed by the microcavity effects dominantly. When the RSL was incorporated into the TOLED, the scattering dominates the internal optical effects. This is accordance with the simulation results, which verified to weaken the microcavity effect due to the RSL. Experimentally, because of the scattering dominancy and mitigated microcavity, it was possible to achieve nearly identical efficiencies with distinguished enhancement in the RSL embedded TOLEDs irrespective of the HTL thickness. In addition, with the use of the RSL it was possible to reduce the viewing angle dependency of EL spectra to a marginal degree. Based on our results, we expect the random nanostructured scattering layer has great potential as an internal light-extracting layer to enhance total efficiency without introducing spectral changes in TOLEDs.

Acknowledgements

This work was supported by IT R&D program of Ministry of Trade, Industry and Energy(MOTIE)/Korea Evaluation Institute of Industrial Technology(KEIT), Rep. of Korea (KI002068 and 10041062, Development of Eco-Emotional OLED Flat-Panel Lighting and Development of Fundamental Technology for Light Extraction of OLED) and the Basic R&D program of ETRI, and IT R&D program of Development of Key Technology for Interactive Smart OLED Lighting, which is a part of ETRI Internal Research Fund from Ministry of Science, ICT and Future Planning(MSIP).

Notes and references

* *OLED Research center, Electronics and Telecommunications Research Institute, Daejeon 305-700, Korea. Fax: +82-42-860-5202; Tel: +82-42-860-0826; E-mail: jiklee@etri.re.kr*

† Electronic Supplementary Information (ESI) available: Simulation result of total (bottom and top) radiance of TOLEDs with the RSL depending on HTL and ETL thickness. See DOI: 10.1039/b000000x/

1 C. F. Madigan, M. H. Lu, J. C. Sturm, *Appl. Phys. Lett.*, 2000, **76**, 1650-1652.
2 A. Chutinan, K. Ishihara, T. Asano, M. Fujita, S. Noda, *Org. Electron.*, 2005, **6**, 3-9.
3 R. Bathelt, D. Buchhauser, C. Gärditz, R. Paetzold, P. Wellmann, *Org. Electron.*, 2007, **8**, 293-299.
4 T. Yamasaki, K. Sumioka, T. Tsutsui, *Appl. Phys. Lett.*, 2000, **76**, 1243-1245.
5 J. M. Lupton, B. J. Matterson, I. D. W. Samuel, *Appl. Phys. Lett.*, 2000, **77**, 3340-3342.
6 J. Sun, S. R. Forrest, *J. Appl. Phys.*, 2006, **100**, 073106/1-073106/6.
7 S. Reineke, F. Lindner, G. Schwartz, N. Seidler, K. Walzer, B. Lüssem, K. Leo, *Nature*, 2009, **459**, 234-238.
8 J. Sun, S. R. Forrest, *Nature Photon.*, 2008, **2**, 483-487.
9 B. J. Matterson, J. M. Lupton, A. F. Safonov, M. G. Salt, W. L. Barnes, I. D. W. Samuel, *Adv. Mater.*, 2001, **13**, 123-127.

10 J. M. Ziebarth, A. K. Saafir, S. Fan, M. D. McGehee, *Adv. Funct. Mater.*, 2004, **14**, 451-456.

11 K. Ishihara, M. Fujita, I. Matsubara, T. Asano, S. Noda, H. Ohata, A. Hirasawa, H. Nakada, N. Shimoji, *Appl. Phys. Lett.*, 2007, **90**, 111114.

12 C. S. Choi, D.-Y.Kim, S.-M. Lee, K. C. Choi, H. Cho, T.-W. Koh, S. Yoo, *Adv. Opt. Mater.*, 2013, **1**, 687-691.

13 J. Y. Kim, C. S. Choi, W. H. Kim, D. Y. Kim, D. H. Kim, K. C. Choi, *Opt. Express*, 2013, **21**, 5424-5431.

14 H. W. Chang, J. Lee, S. Hofmann, Y. H. Kim, L. M.-Meskamp, B. Lüssem, C.-C. Wu, K. Leo, M. C. Gather, *J. Appl. Phys.*, 2013, **113**, 204502.

15 H. W. Chang, J. Lee, T.-W. Koh, S. Hofmann, B. Lüssem, S. Yoo, C.-C. Wu, K. Leo, M. C. Gather, *Laser & Photonics Rev.*, 2013, 1-9.

16 J.-W. Shin, D.-H. Cho, J. Moon, C. W. Joo, S. K. Park, J. Lee, J.-H. Han, N. S. Cho, J. Hwang, J. W. Huh, H. Y. Chu, J.-I. Lee, *Org. Electron.*, 2014, **15**, 196-202.

17 J.W. Huh, J. Moon, J.W. Lee, D.-H. Cho, J.-W. Shin, J.-H. Han, J. Hwang, C.W. Joo, H.Y. Chu, J.-I. Lee, *IEEE Photonics J.*, 2012, **4**, 39-47.

18 J. Moon, J. W. Huh, C. W. Joo, J.-H. Han, J. Lee, H. Y. Chu, J.-I. Lee, SPIE Newsroom (7 November 2013), DOI: 10.1117/2.1201310. 005197/1-005197/3.

19 J.-I. Lee, J. Lee, J.-W. Lee, D.-H. Cho, J.-W. Shin, J.-H. Han, H. Y. Chu, *ETRI J.*, 2012, **34**, 690-695.

20 K.A. Neyts, *J. Opt. Soc. Am. A.*, 1998, **15**, 962-971.

21 M. Furno, R. Meerheim, M. Thomschke, S. Hofmann, B. Lussem, K. Leo, *Proc. of SPIE.*, 2010, **7617**, 761716/1-761716/12.

22 K. S. Yee, *IEEE Trans.Antennas Propagat.*, 1966, **AP-14**, 302-307.

23 A. Chutinan, K. Ishihara, T. Asano, M. Fujita, S. Noda, *Org. Electron.*, 2005, **6**, 3-9.

24 H. Haidner, D. Dias, L. L. Wang and T Tschudi, *Pure Appl. Opt.*, 1998, **7**, 1347-1361.

25 A. Gombert, K. Rose, A. Heinzel, W Horbelt, C. Zank, B. Blasi, V. Wittwer, *Solar Energy Materials and Solar Cells*, 1998, **54**, 333-342.

26 M. Thomschke, R. Nitsche, M. Furno, K. Leo, *Appl phys lett.*, 2009, **94**, 083303.

27 A. Dodabalapur, L. J. Rothberg, T. M. Miller, and E. W. Kwock, *Appl. Phys. Lett.*, 1994, **64**, 2486-2488.

28 A. Dodabalapur, L. J. Rothberg, R. H. Jordan, T. M. Miller, and R. E.Slusher, and Julia. M. Phillips, *J. Appl. Phys.*, 1996, **80**, 6954-6964.

29 E. Wolf, *J. Opt. Soc. Am.* 1978, **68**, 6-17.

30 A. Epstein, N. Tessler, P. D. Einziger, PIERS Online, 2009, **5**, 75-80.

31 H. Cho, C. Yun, S. Yoo, *Opt.express.*, 2010, **18**, 3404-3414.

32 D. G. Deppe, C. Lei, C. C. Lin, and D. L. Huffaker, *J. Mod. Opt.*, 1994, **41**, 325-344.